

Arc Characteristics and a Single-Pole Auto-Reclosure Scheme for Alexandria HV Transmission System

A.I. Megahed¹, H.M. Jabr², F.M. Abouelenin¹ and M.A. Elbakry²

(1) Electrical Engineering Department, Alexandria University, Alexandria, Egypt (e-mail: amegahed@dataxprs.com.eg), (2) High Voltage Department, Electronics Research Institute, Dokki, Giza, Egypt (e-mail: hanyjabr@engineer.com)

Abstract – Arcing faults are the most common faults that occur in the 220kV transmission line national grid of Egypt, in the vicinity of ‘Alexandria’ city. This part of the network also feeds a large industrial load in the form of steel works, which injects a large amount of harmonics into the network. In this paper the performance of this 220kV TL network during arcing faults is studied with the aid of the PSCAD/EMTDC program together with a specially designed arcing fault custom model incorporated in the program. Several arcing faults are simulated, and the effect of harmonics on the fault current and secondary arc duration time is demonstrated. Based upon the simulation results, recommendations regarding single-pole autoreclosing and arc suppression methods are suggested.

Keywords – Arcing fault, Transient analysis, Harmonic analysis, Autoreclosure.

I. INTRODUCTION

There is an increasing demand for more detailed and accurate modeling techniques for predicting the transient response of EHV transmission systems caused in particular by arcing faults which constitute, by far, the largest proportion of faults on such systems [1]. This is particularly so in relation to the design and development of alternative and improved equipment such as adaptive autoreclosure schemes and new protection techniques. An accurate prediction of the fault transients requires a detailed and comprehensive representation of all the components in a system, and the transient studies have to be conducted into the frequency range well above the normal power frequency.

From a modeling point of view, the fault arc can be classified into the primary arc during fault duration (before breakers open) and the secondary arc which occurs after the breakers trip, and which is maintained by the mutual coupling between the faulted phase and the sound phases. It has been a long tradition that the primary arc can be simply represented by an ideal short circuit or by a low value linear resistance. However, if the transients produced by arcing faults are to be predicted with precision, the fault arc has to be represented as accurately as possible. Recently, it has been suggested that the theory of the switching arc could be applied to model an unconstrained long fault arc in air, including the primary and the secondary arcs [2]. In this paper the arcing fault is represented by a time dependent dynamic resistance model which is based on the switching arc theory [3]. The arcing model is incorporated as a custom model in the PSCAD/EMTDC program [4]. The algorithm and its inclusion in the PSCAD/EMTDC pro-

gram, as used in this paper, is explained in detail in [5].

The 220kV transmission line national grid of Egypt, in the vicinity of ‘Alexandria’ city, suffers from recurring occurrence of single-phase arcing faults in the early hours of the morning due to the high humidity in the atmosphere. Moreover, there exists a large industrial complex (average load 150 MW) in the form of steel works that is fed directly from the 220kV network and which injects a large amount of harmonics into the network due to its installed arc furnaces. The combined effect of arcing faults and harmonic injection has an adverse effect on the HV network. It is the aim of this paper to study the combined effect of arcing faults and harmonics on the 220kV transmission line network in the vicinity of ‘Alexandria’. The arcing faults will be simulated using the PSCAD/EMTDC program together with the arcing fault custom model [5]. The currents of the network including the fault current will be analyzed and abnormal effects on the network will be pointed out.

II. ARCING FAULT MODEL

This section presents an overview of the arcing fault equations that constitute the model.

A. Arcing Fault Algorithm

1) Primary Arcs:

As far as the primary arc is concerned, it can be assumed to behave similar to the constrained switching arc because there is no obvious elongation of the arc length and a relatively large cross-section is involved. In this sense, the switching arc theory can be applied to primary arc modeling. Hence, arcing fault is represented by a time dependent resistance with value given by [2], [3]:

$$\frac{dg_p}{dt} = \frac{I_p}{2.85 \times 10^{-5} I_p} \left(\frac{|i|}{15I_p} - g_p \right) \quad (1)$$

where g_p is the time varying primary arc conductance, I_p is the peak value of primary arc current, I_p is the primary arc length and $|i|$ is the absolute value of the primary arc current.

2) Secondary Arcs:

As far as long arcs are concerned, when the arc is conducting, almost all of the total arc voltage appears across the main arc column [6]. To a very good degree of approximation, the voltage drop near the arcing horns can be neglected. Various experimental studies have confirmed

that the voltage drop along the main arc column is substantially independent of current, and that for much of the AC cycle the voltage drop per unit length is nearly constant [6], [7]. It follows that the total secondary arc voltage is practically proportional to the arc length, which in turn varies with time. The main factors influencing the arc length variation are wind velocity and the magnitude and duration of the preceding primary fault arc current. The secondary arc is a highly complex phenomenon, and is influenced by a number of factors. The overall effects of the extremely complex processes, associated with arc voltage reversals, are to cause successive partial arc extinctions and restrikes that may be repeated many times as the arc current and voltage pass through zero, with permanent extinction finally occurring when the arc reignition voltage exceeds the voltage impressed across the discharge path [8].

A previous study of the secondary arc characteristics [3], [7] has shown that such characteristics can be exactly simulated by the following:

$$\frac{dg_s}{dt} = \frac{l_s(t_r)}{2.51 \times 10^{-3} I_s^{1.4}} \left(\frac{|i|}{75 I_s^{0.4} l_s(t_r)} - g_s \right) \quad (2)$$

where g_s is the time varying secondary arc conductance, I_s is the peak value of the secondary arc current, l_s is the secondary arc length and t_r is the time from the initiation of the secondary arc.

It has been shown in [3] that, following arc-path voltage reversal, the arc current is held at zero for as long as the arc voltage magnitude remains below the value obtained from (3).

$$v_r(t_r) = \left[5 + \frac{1620T_e}{2.15 + I_s} \right] (t_r - T_e) h(t_r - T_e) \times 10^3 \quad \text{V/cm} \quad (3)$$

where $v_r(t_r)$ is the arc reignition voltage that has to be reached before the arc restrikes again, T_e is time from the initiation of secondary arc to a current zero and $h(t_r - T_e)$ is a delayed unit-step function ($= 0$ when $t_r < T_e$, $= 1$ when $t_r > T_e$).

In practice, the secondary arc extinction time also depends on the rate of rise of the secondary arc path length, which, in turn, is heavily dependent upon the wind velocity. The increase in typical secondary arc lengths as a function of time can be approximated by (4) for relatively low wind velocities from 0-1 m/s [9].

$$l_s(t_r)/l_{s0} = \begin{cases} 1 & \text{for } t_r \leq 0.1 \text{ s} \\ 10t_r & \text{for } t_r > 0.1 \text{ s} \end{cases} \quad (4)$$

III. ALEXANDRIA 220KV TL NETWORK

The single line diagram of the 220kV network under study is shown in Fig. 2. The network is connected to the national grid at ‘Abis’ and ‘El Amria’ locations with short-circuit levels of 4 GVA and 4.5 GVA respectively. At ‘AbuKir’ location there exists a generating plant with a full capacity of 900 MW and a short-circuit level of 9.5 GVA at its busbar that links it with the national grid. The indus-

trial area, ‘El Hadeed wel solb’, that is formed of a large steel works has a load with an average value of 150 MW and a maximum of 200 MW. The steel works has among its load 4 arc furnaces each of rating 46 MVA and two ladle furnaces each of rating 15 MVA. A filter is installed on the same busbar with the arc furnaces to absorb the harmonics produced by the furnaces. An actual daily load curve for the steel works, ‘El Hadeed wel solb’, is shown in Fig. 2(a) and the current and voltage Total Harmonic Distortion (THD) variation are shown in Figs. 2(b) and 2(c) respectively. The curves of Figs. 2(a), 2(b) and 2(c) represents actual measurements recorded at the steel works busbar using a harmonic analyzer for a period of 24 hours. Also these measurements represent more or less a repeated pattern for the daily load cycle and its associated THD variation. Figure 2(d) shows the current harmonic spectrum at maximum VTHD and Fig. 2(e) shows the voltage harmonic spectrum at maximum VTHD.

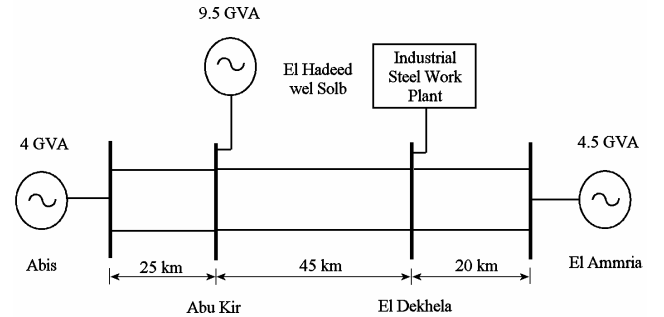


Fig. 1: The Single line diagram of ‘Alexandria’ 220kV network.

The normal operating condition of the TL network, Fig. 1, is with ‘Abis’ operating as a sending end source, ‘AbuKir’ operating at its full generating capacity, around 900 MW, while ‘El Amria’ is a receiving end source. The industrial plant, ‘El Hadeed wel solb’, is considered as a continuous 24 hour load with an average daily load curve as indicated in Fig. 2(a) and with harmonic percentages as indicated in Figs. 2(b)-2(e). However, there are certain periods of the year in which the plant is closed for maintenance, during these periods the plant is considered to be switched off.

Figure 3 shows the TL network under study, shown in Fig. 1, as implemented in PSCAD/EMTDC together with the developed custom defined arcing fault model. There are three distributed transmission line models available in PSCAD/EMTDC program [4], the Bergeron model, the frequency dependent (Mode) model and the frequency dependent (Phase) model. The frequency dependant (Phase) model uses curve fitting to duplicate the frequency response of a line. It is the most advanced time domain model available on any simulator as it represents the full frequency dependence of all line parameters (including the effect of a frequency dependant transform). It is useful for studies wherever the transient or harmonic behavior of the line is important [10]. Hence, the frequency dependent phase model is used through out the work presented in this paper.

The arcing fault module is responsible for simulating both the primary and secondary arcing faults as explained in detail in [5]. There are two types of inputs to the module,

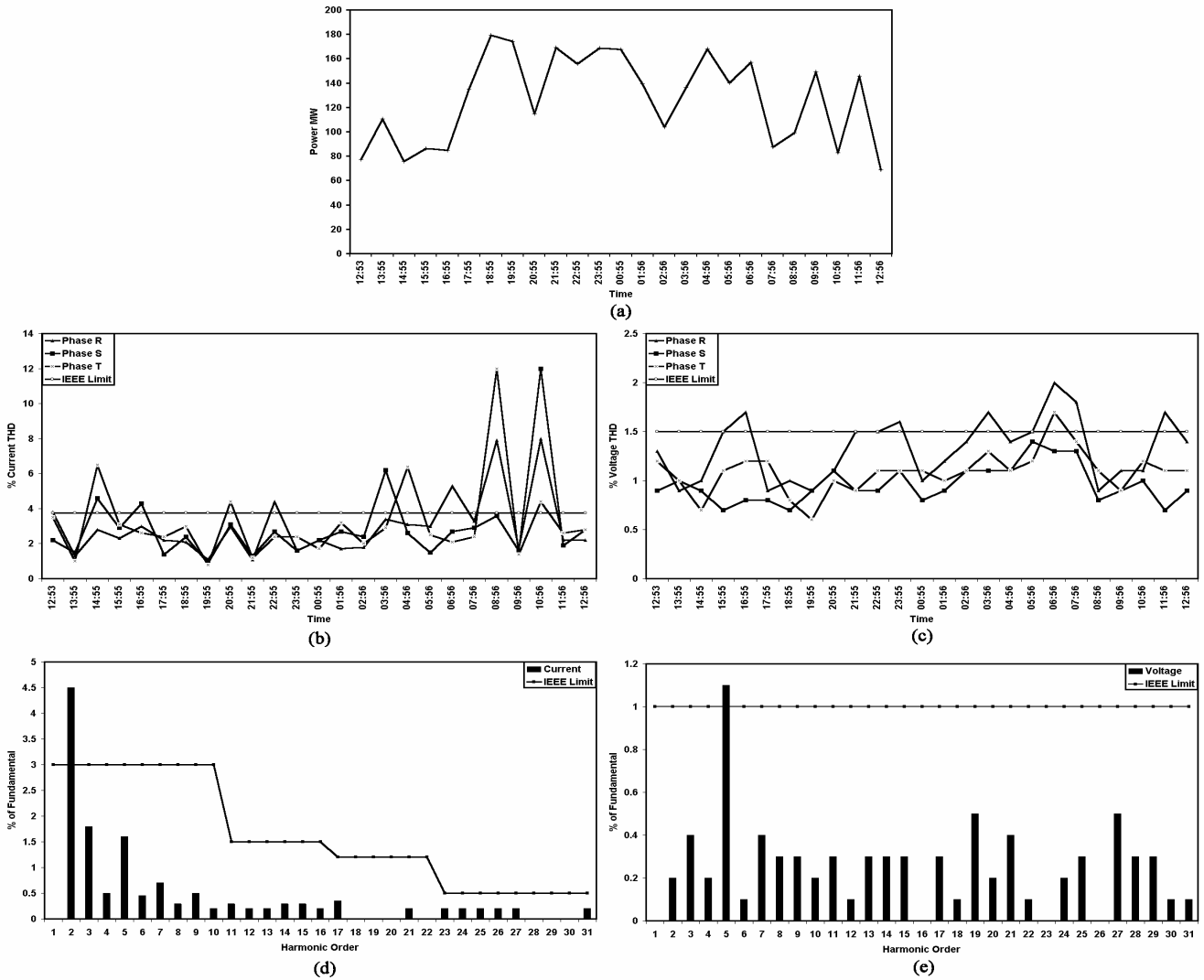


Fig. 2: Industrial plant load data. (a) Industrial plant daily load curve. (b) Current THD variation. (c) Voltage THD variation. (d) Current Harmonic Spectrum. (e) Voltage Harmonic Spectrum.

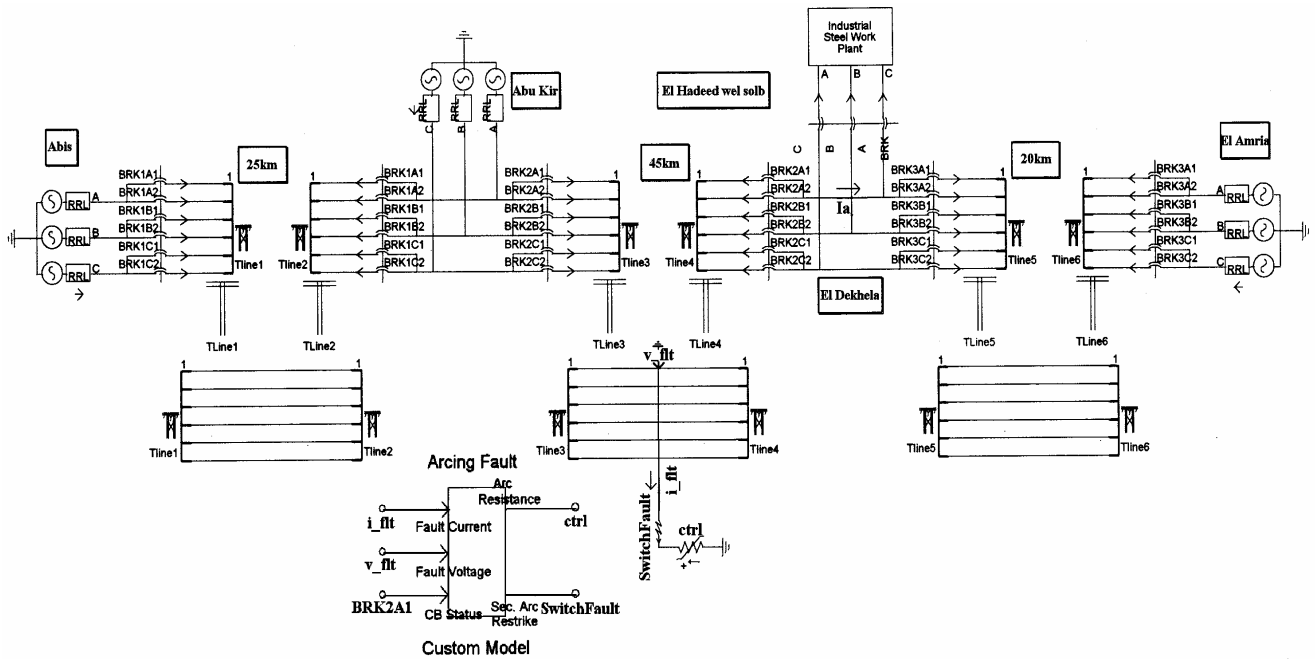


Fig. 3: PSCAD/EMTDC Alexandria network representation.

the constant inputs and the instantaneously variable inputs. The constant inputs are the peak value of the primary arc current, I_p , the peak value of the secondary arc current, I_s , the primary arc length, l_p , and the time of fault inception [2], [3]. The variable inputs to the module are the instantaneous values of the fault current, i_{flt} , fault voltage, v_{flt} , and the circuit breaker status (closed indicates primary arc simulation and opened indicates secondary arc simulation). The outputs of the module are the value of the time dependent arcing fault resistance, $ctrl$, and a fault switch which controls the extinction (open) or reignition (close) of the secondary arc conducting characteristics.

The harmonics of the load are represented in PSCAD/EMTDC by harmonic injecting current sources as shown in Fig. 4. The percentages of the harmonic currents injected are relative to the load of the industrial plant as indicated in the curves of Fig. 2(d).

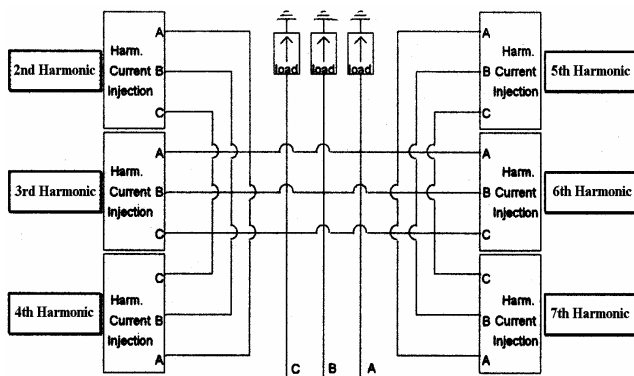


Fig. 4: Load harmonics representation in PSCAD/EMTDC.

IV. ARC CHARACTERISTICS

The aim of this section is to study the arcing fault characteristics of the 220kV TL network shown in Fig. 1 by means of the PSCAD/EMTDC model shown in Fig. 3. Several arcing faults are simulated at various fault locations and loading levels. The purpose of studying the arc characteristics is to reach conclusions regarding the operating strategy of the network in terms of applying autoreclosing techniques for single phase faults and applying arc suppression methods. Also it is required to study the effect of harmonics on the arc extinction time.

The arcing fault module is used to simulate the primary arc followed by the secondary arc on the system shown in Fig. 3 for an arc length of 70 cm at mid point of phase a for one of the parallel transmission lines, i.e. fault is on one of the transmission lines connecting ‘AbuKir’ and ‘El Hadeed wel solb’. The results are shown in Fig. 5. The fault inception time is 0.1s that is when the primary arc starts. When the fault detection and clearing relay operates to open the faulted phase, the secondary arc starts at 0.2s and continues until the final extinction occurs at 0.35s. The primary arc resistance is in the range of 0.11Ω to 0.16Ω as shown in Fig. 5(d). The effect of arc elongation, due to wind effect, is obvious on the non-linear arc resistance which starts to increase after 0.1s from secondary arc initiation as shown in Fig. 5(e).

The effect of the harmonic feeding load, ‘El Hadeed wel solb’, on the network during the arcing faults can best be presented by analyzing the frequency spectrum for the current I_a , Fig. 3, (I_a is the current feeding ‘El Hadeed wel solb’ from the S.E. ‘Abis’) once with the load switched on, Fig. 6(a), and another time with the load switched off, Fig. 6(b). The fault inception time for both cases is 0.2s, the circuit breakers operate to open the faulted phase at both ends at 0.4s, the secondary arc extinguishes at 0.5357s for both faults, that confirms with the results shown later in Fig. 7. It should be noticed that single-pole breaker opening is applied only to the faulted phase at both ends of one of the transmission lines while the parallel healthy transmission line is still in service. Comparing the frequency spectrum of Figs. 6(a) and 6(b), in particular from the instant of fault inception until breaker opening, it can be seen that the load case causes slightly higher harmonic values at fault inception and breaker opening instants. Moreover, during the intermediate period between fault inception and breaker opening, the load causes higher harmonic ripples than the no-load case. As the values of the secondary arc current is very small, the harmonics are almost negligible, however, it can still be seen that the load current contains harmonics, while the no-load case does not.

The effect of harmonics on secondary arc duration is presented in Fig. 7, showing the secondary arc duration versus fault location (fault location is measured from the S.E. at ‘Abis’) for an arc length of 70 cm. Two cases are shown in Fig. 7, one case for the load case and the other is when the industrial plant, ‘El Hadeed wel solb’, is switched off. At the latter case, the harmonic level in the network is almost negligible. It should be noticed that for the two cases the current at the sending end is maintained the same, i.e. the only difference between the load case and no-load case is the percentage of harmonics in the network. Comparing the two cases shown in Fig. 7, it can be seen that the effect of harmonics is slightly decreasing the secondary arc duration. This can be attributed to the damping effect of the high percentage of second harmonic current as shown in Fig. 2(d). However, it was expected that harmonics cause an increase in secondary arc duration time. Further study is underway in order to reach a more general conclusion on the effect of different harmonic percentages on secondary arc duration.

The fault arc must span two electrodes, the overhead line and some other mechanical object that provides a path to earth. There is a range of mechanical structures that can carry the fault current to earth and these include humid insulators, metal towers and wooden trees. Hence, several arc lengths are obtained based upon the nature of the mechanical object as indicated in [11]. Figure 8 shows the arc characteristics of the network. The secondary arc duration is plotted versus the fault location for different arc lengths with the load switched on. It can be seen from Fig. 8 that the secondary arc duration is higher for the faults occurring on the transmission line connecting ‘AbuKir’ to ‘El Hadeed wel solb’, Fig. 3. However, the secondary arc duration is relatively small, as it has never exceeded 150ms. The short arc duration can be attributed to the relatively short trans-

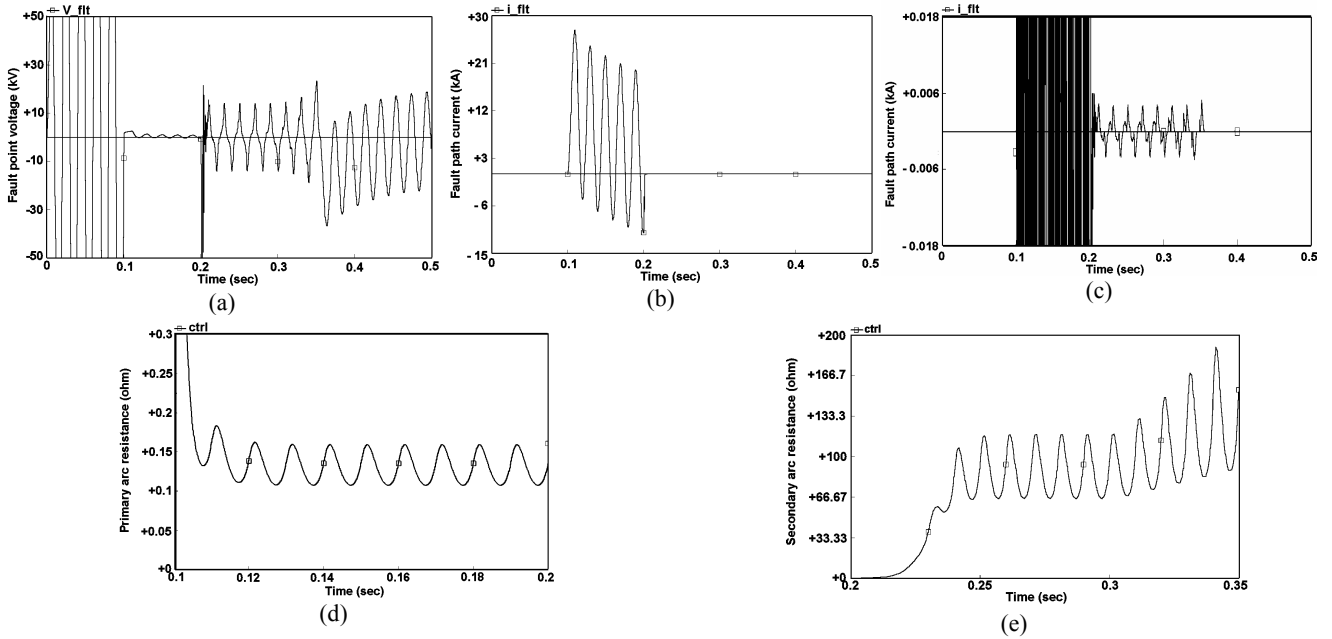


Fig. 5: The results of a typical case for an arcing fault at the middle of one TL connecting ‘AbuKir’ and ‘El Hadeed wel solb’.
 (a) Fault voltage. (b) Primary arc current. (c) Secondary arc current. (d) Primary arc resistance. (e) Secondary arc resistance.

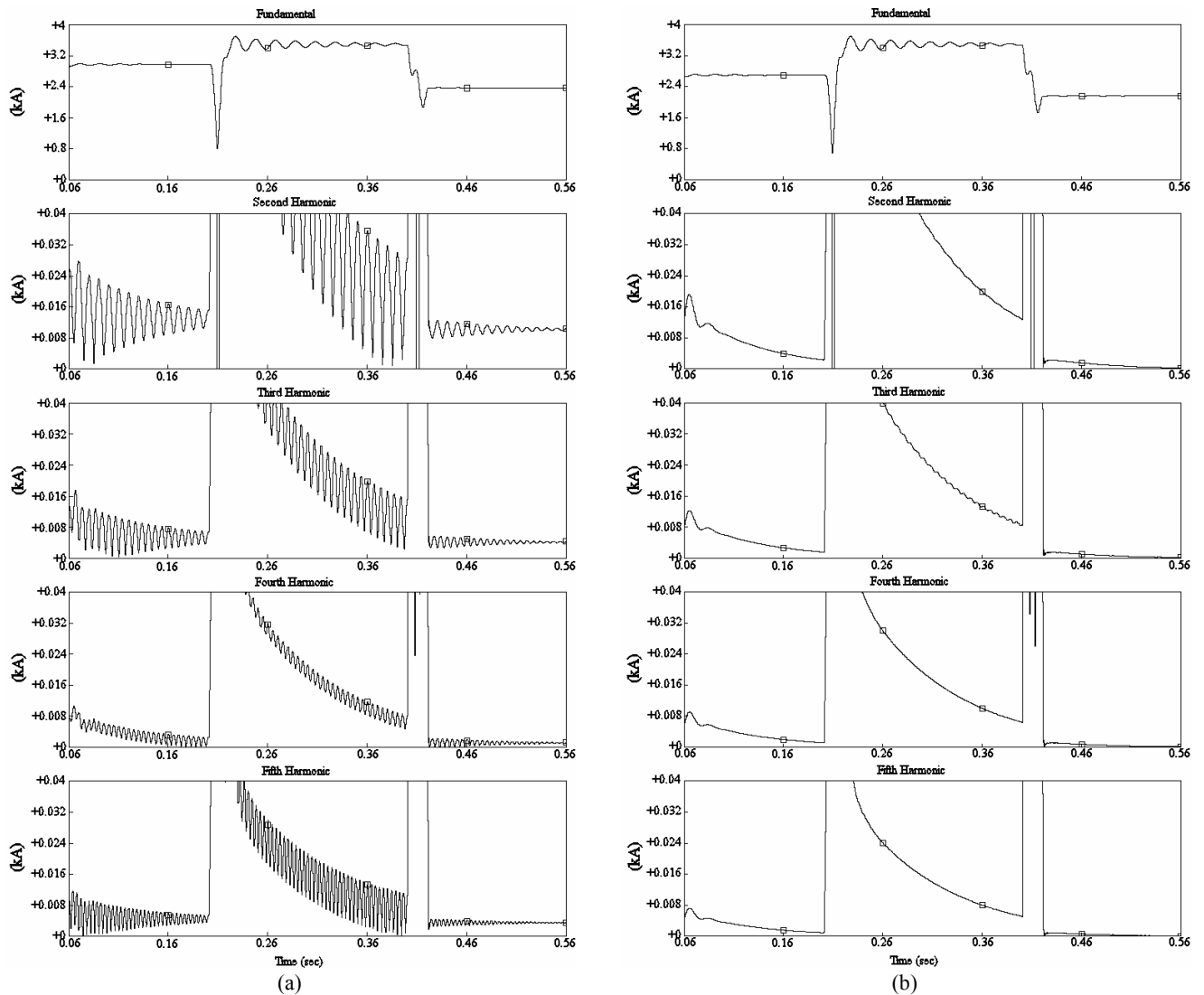


Fig. 6: Harmonic analysis of network current.
 (a) Load switched on.

(b) Load switched off.

mission lines, which does not maintain the secondary arc. Also it is noticed that towards the receiving end the arc duration is minimum.

In view of all previous simulations, Figs. 5-8, showing the arc behavior in the 220kV TL network in the vicinity of ‘Alexandria’ in the presence of a load with relatively high harmonic percentages, several conclusions can be reached. At first it can be noticed that the currents in the network contain a higher harmonic ripple during fault condition, with a slight increase in the harmonic value during fault inception and breaker opening. The relatively short secondary arc duration time, in the range of 100-150ms, makes the network in no need for arc suppression methods, as four-reactor bank, high speed grounding switch and hybrid single-phase scheme [1], that speed up arc extinction. Automatic single-pole reclosing, of the faulted phase, can be safely applied after a period of 200ms from the first breaker opening, this period is also known to be the dead time of the circuit breaker.

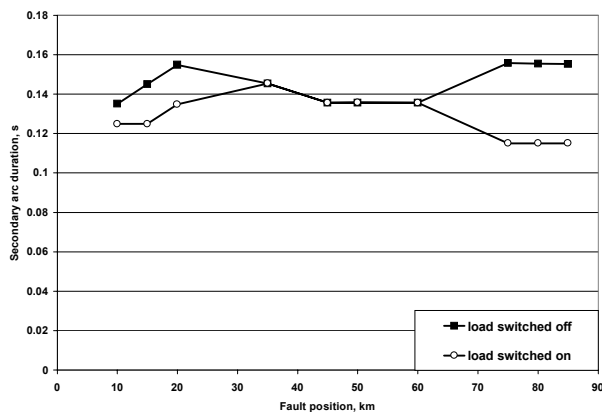


Fig. 7: Effect of harmonics on secondary arc duration.

V. CONCLUSIONS

The 220kV TL network in the vicinity of ‘Alexandria’ city is implemented in the PSCAD/EMTDC program together with a previously developed custom defined arcing fault model. The PSCAD/EMTDC model is used to study the arcing characteristics of the network in the presence of a large industrial load that contains relatively high harmonic percentage. The frequency spectrum of the network currents is analyzed during the fault and it is seen that there is an increasing harmonic ripple when the load is switched on but with no significant damaging effects. It is noticed that the harmonics decrease the period of the secondary arc. Further study is in progress to obtain a more generalized conclusion on the effect of harmonics on secondary arc duration time. It is also concluded that automatic reclosing of the faulted phase can be practiced in this network, where arcing faults are common to occur, with closing times in the range of 200ms from first breaker opening. Hence, the relatively high-speed autoreclosing scheme that can be implemented in this network will significantly improve its stability and reliability.

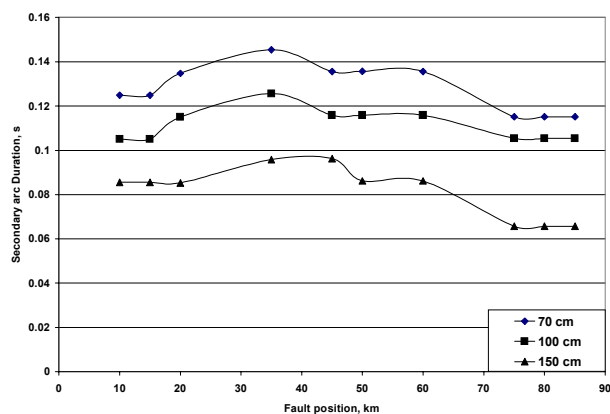


Fig. 8: Effect of arc length and fault location on the secondary arc duration in the presence of harmonics.

REFERENCES

- [1] Members of the IEEE Power System Relaying Committee, “Single phase tripping and auto reclosing of transmission lines”, IEEE Trans. on Power Delivery, Vol. 7(1), pp.182-192, 1992.
- [2] Kizilcay, M., and Pniok, T.: “Digital simulation of fault arcs in power system”, European Trans. on Electrical Power, Vol. 1(1), pp. 55-60, 1991.
- [3] A.T. Johns, R.K. Aggarwal, and Y.H. Song, “Improved techniques for modeling fault arcs on faulted EHV transmission systems”, IEE Proc. Gener. Transm. Distrib., Vol. 141(2), pp. 148-154, 1994.
- [4] Manitoba HVDC Research Center, PSCAD/EMTDC Power Systems Simulation Software Manual, MB., Canada, 1997.
- [5] A.I. Megahed, H.M. Jabr, F.M. Abuelenin, and M.A. Elbakry, “PSCAD/EMTDC arcing fault custom model and a novel adaptive single-pole autoreclosure scheme”, Electric Power and Energy Systems, paper submitted in October 2002.
- [6] T. E. Browne, "The electric arc as a circuit element," Journal of Electro-Chemical Society, Vol. 102, pp. 27-37, 1955.
- [7] A. P. Strom, "Long 60 cycle arcs in air," Trans. Am. Inst. Elec. Eng., Vol. 65, pp. 113-117, 1946.
- [8] A. T. Johns, and A. M. Al-Rawi, "Digital simulation of EHV systems under secondary arcing conditions associated with single-pole autoreclosure," IEE Proc. Part C, Vol. 129, pp. 49-58, 1982.
- [9] K. Anjo, H. Terase, and Y. Kawaguchi, "Self-extinction of arcs created in long air gaps," Electrical Engineering Japan, Vol. 88, pp. 83-93, 1968.
- [10] A.B. Fernandes, W. Neves, E.G. Costa, and M.N. Cavalcanti, “The effect of the shunt conductance on transmissionline models”, International Conference on Power system transients IPST '01, Rio de Janeiro, Brazil, June 24-28, 2001.
- [11] D.L. Hickery, E.J. Bartlett, and P.J. Moore, “Investigation into physical and electrical processes of power system fault arcs”, Proc. 34th Universities Power Engineering Conference (UPEC99), Vol. 2, pp. 575-578, Sept. 1999.